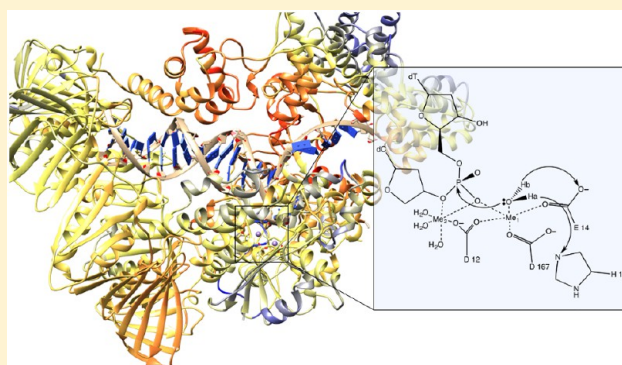


## Computational Simulations of DNA Polymerases: Detailed Insights on Structure/Function/Mechanism from Native Proteins to Cancer Variants

Alice R. Walker<sup>1</sup> and G. Andrés Cisneros<sup>1\*</sup>

Department of Chemistry, University of North Texas, 1155 Union Circle, Denton, Texas 76203, United States

**ABSTRACT:** Genetic information is vital in the cell cycle of DNA-based organisms. DNA polymerases (DNA Pols) are crucial players in transactions dealing with these processes. Therefore, the detailed understanding of the structure, function, and mechanism of these proteins has been the focus of significant effort. Computational simulations have been applied to investigate various facets of DNA polymerase structure and function. These simulations have provided significant insights over the years. This perspective presents the results of various computational studies that have been employed to research different aspects of DNA polymerases including detailed reaction mechanism investigation, mutagenicity of different metal cations, possible factors for fidelity synthesis, and discovery/functional characterization of cancer-related mutations on DNA polymerases.



### CONTENTS

1. Introduction	1922
2. Computational Investigation of DNA Polymerase Reaction Mechanisms	1923
2.1. Third Metal in Pol $\lambda$ Mechanism	1925
3. Metal Mutagenicity in DNA Polymerases	1926
4. DNA Synthesis Fidelity Checking	1927
5. Effects of Mutagenic Lesions on Structure and Function of DNA Polymerase IV	1929
6. Discovery and Characterization of Cancer Mutants on DNA Pols	1929
7. Summary and Perspective	1931
Author Information	1931
Corresponding Author	1931
ORCID	1931
Funding	1932
Notes	1932
Biographies	1932
Acknowledgments	1932
Abbreviations	1932
References	1932

### 1. INTRODUCTION

The accurate synthesis and maintenance of DNA in cells depend heavily on a complex network of proteins, of which DNA polymerases are crucial players. Each DNA polymerase has a unique task to ensure the successful replication and repair of the genome of a cell. The number of potential errors, mismatches, and damage to DNA is vast, with far-reaching

consequences for cell function that can result in disease or, in many cases, death.<sup>1–4</sup> These polymerases have complex structures, mechanisms, and dynamics, which in many cases are not fully understood.<sup>5–7</sup> Computational investigations of these systems require a variety of techniques and a balance between rigorous theory and computational resources, especially considering the relatively large size of polymerase systems and their multifarious functions.<sup>8</sup>

DNA polymerases are divided into several families, each of which has similarities in active site structure, processivity, and potential for additional activity (such as exonuclease or lyase capabilities).<sup>9–12</sup> In brief, family A polymerases perform excision repair with relatively poor processivity; family B performs DNA repair with the potential to bypass lesions and has variable processivity; family C performs DNA synthesis with a proofreading function and a high level of processivity; family X is involved several types of DNA repair, including base excision repair (BER) and non-homologous end joining (NHEJ); and family Y performs translesion DNA synthesis with a low level of accuracy.<sup>8,13–15</sup>

Even within families there can be substantial differences in structure and function of the various polymerases. However, overall the polymerase subdomain structures are generally similar and are usually described as a right or left-hand. Within

**Special Issue:** DNA Polymerases: From Molecular Mechanisms to Human Disease

**Received:** June 7, 2017

**Published:** September 6, 2017

the hand there are the finger, thumb, and palm domains. The palm domain is where the DNA is bound while the polymerase is active, and also where the active site for phosphoryl transfer/nucleotide addition takes place, which is discussed more thoroughly below. The thumb domain is usually thought to be involved in the position and movement of the DNA through the polymerase, and the finger domain is involved with the alignment of the incoming nucleotide with the template strand and, potentially, recognition of the correct incoming nucleotide.<sup>16</sup>

Computational simulations based on detailed classical and/or quantum analysis have been applied to gain atomic-level insight into this important class of enzymes. Molecular dynamics (MD) simulations allow for the investigation of large and small-scale structural differences over time and can provide better understanding regarding how large, flexible polymerases adapt to relatively small structural changes, such as mutagenic lesions, and how they maintain fidelity.<sup>17–21</sup> These simulations can also provide information on large scale motions and structural changes such as switching between polymerase and exonuclease activities.<sup>22,23</sup> As a recent example, Kim et al. have provided a novel explanation for how DNA polymerase  $\beta$  (Pol $\beta$ ) becomes inactivated by oxidized guanine by applying targeted MD to obtain the specifics of the transition from the open active state of Pol $\beta$  to the inactive closed state by disruption of a water network and, eventually, the active site.<sup>24</sup> Yang et al. have also used targeted MD to investigate how Pol $\beta$  changes between correctly paired terminal bases versus incorrectly paired ones, and show aspects of the overall motion of Pol $\beta$ , and of a rotation of Arg258 in the active site that has been correlated to the shift from the active to inactive state.<sup>25</sup> Additionally, molecular mechanics (MM) work by Jia et al. uncovered the N-clasp structural feature of Pol $\kappa$  that allows for nearly error-free bypass of mutagenic lesions.<sup>26</sup>

Quantum mechanical (QM) and hybrid QM/molecular mechanics (QM/MM) methods have also frequently been used to investigate polymerase function and activity. QM methods alone are highly accurate but are difficult or impossible to apply to large enzymatic systems, and so usually QM/MM is used to obtain information on the complex electronic structure of the metal ions and accurate energetics for reaction mechanisms.<sup>7,27–30</sup> QM/MM subdivides the calculated system into a small region of 100 atoms or less that is calculated with QM, usually the active site of the polymerase along with relevant ions and cofactors, and the MM region, containing the rest of the polymerase and solvent. This allows for insight into particulars of the reaction mechanisms and metal catalysis that differ between specific polymerase families and sometimes within polymerases themselves, as discussed further in section 2 and throughout the perspective. These cannot be investigated with MD alone since they require investigation into bond breaking and forming and the movement of electrons. Family X and Y polymerases in particular have been the object of a large number of QM/MM<sup>31</sup> simulations.<sup>19,32–39</sup> To name a few examples, Hummer et al. have applied combined QM/MM techniques to investigate a variety of aspects about *B. halodurans* ribonuclease (RNase), including the reactivity of specific metals and the overall mechanism, gaining insights into nucleotide cleavage and transfer reactions.<sup>40</sup> Combined QM/MM simulations and structural/biochemical experiments, reported by Perera et al., have given fascinating insight into the role of metal ions in the active site of Pol $\beta$ , and their dynamics of facilitation and inhibition in relation to

pyrophosphorolysis, or the reverse of the usual addition reaction of polymerases.<sup>41</sup> QM/MM has also been used to gain mechanistic insight into several Y family polymerases, which are unique in their ability to bypass bulky chemical lesions. Dpo4, which can perform error-prone translesion synthesis, has a particularly solvent-exposed active site; Wang et al. have shown a corresponding mechanism for nucleotidyl-transfer reactions through water-dependent pathways using QM/MM calculations.<sup>42</sup> Additionally, QM/MM work by Hoffmann et al. shows a similar water-mediated transfer reaction for Pol $\kappa$ , which has a much higher fidelity as compared to Dpo4.<sup>43</sup> Further discussion of mutagenic lesions and Dpo4 is found later in the perspective in section 5.

The use of advanced force fields for classical or QM/MM simulations applied to complex biomolecular systems also provides new insights and results, showing new avenues for exploring the role of electronic polarization and improved treatments of permanent electrostatics.<sup>44–48</sup> These advanced methods can improve solvent boundaries for QM/MM<sup>49</sup> and the description of metal cations.<sup>50–52</sup>

We have developed a variety of methods for simulations and analysis, which have been applied to various biochemical systems including DNA polymerases. In this perspective, we discuss our studies on DNA polymerase catalysis in section 2, metal mutagenicity in section 3, fidelity determinants in section 4, mutagenic lesion bypass in section 5, and cancer mutations and their effects on the structure and function of polymerases in section 6.

## 2. COMPUTATIONAL INVESTIGATION OF DNA POLYMERASE REACTION MECHANISMS

As briefly touched on in the Introduction, DNA polymerases possess a remarkable degree of specificity and variability in function. That said, the reaction mechanism of DNA synthesis is very consistent across polymerases. The reaction mechanism for DNA synthesis by DNA polymerases involves a nucleophilic attack on the alpha phosphate (P $\alpha$ ) of the incoming nucleotide by the O3' of the primer-terminus nucleotide with the concomitant formation of pyrophosphate (PPi). This reaction results in the formation of an O–P bond and therefore the addition of the incoming nucleotide, as shown schematically in Figure 1. In general, this mechanism is considered to have two metal ions, though that can vary, as will be discussed later in the perspective.<sup>53</sup>

Several reaction mechanisms have been investigated to assess the particulars of proton transfer from the O3' and seem to vary depending on the particular DNA polymerase. The proton transfer from the nucleophilic O may involve a direct proton transfer to an oxygen on the P $\alpha$ , indirectly through an ordered water, or to one of the conserved aspartate/glutamic acid residues in the active site.<sup>36,37,55</sup> We have performed various theoretical studies on the reaction mechanism of DNA polymerase  $\lambda$  (Pol $\lambda$ ).<sup>56</sup> Pol $\lambda$  is an X family polymerase involved in NHEJ and can fill small DNA gaps (1–2 nucleotides). QM/MM simulations of the reaction mechanism for the three H<sup>+</sup> transfer possibilities in Pol $\lambda$  suggest that in this case the proton is transferred to the conserved D490 in the active site.<sup>56</sup>

DNA polymerases have been shown to be able to perform their catalytic activity using different divalent cations in the active site.<sup>4,57</sup> Pol $\lambda$  can employ either Mn<sup>2+</sup> or Mg<sup>2+</sup> to synthesize DNA.<sup>58</sup> We performed QM/MM simulations using both metal cations to determine the differences in the reaction mechanism in Pol $\lambda$ . Our results show that the energy barriers

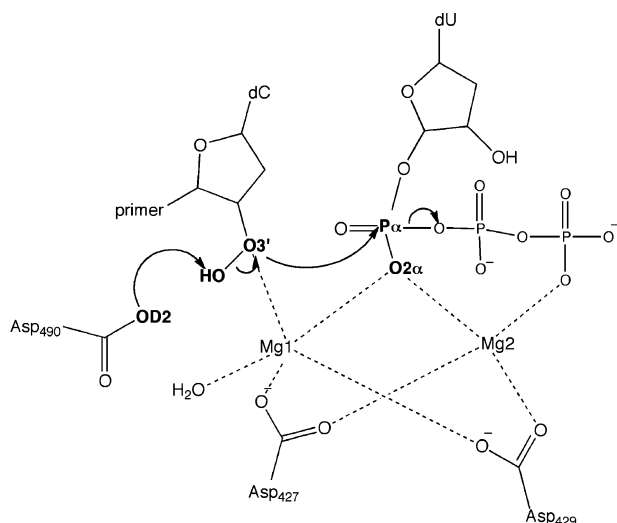


**Figure 1.** Mechanism of polymerase addition reaction for Pol  $\lambda$ . Reproduced from Fang, D., Chaudret, R., Piquemal, J.-P., and Cisneros, G. A. (2013) Toward a Deeper Understanding of Enzyme Reactions Using the Coupled ELF/NCI Analysis: Application to DNA Repair Enzymes. *J. Chem. Theo. Comp.* 9, 2156–2160. Copyright 2013 American Chemical Society.<sup>54</sup>

for both  $Mn^{2+}$  and  $Mg^{2+}$  are in good agreement with experimental estimates.<sup>56</sup> In both cases, the reaction is calculated to proceed through a two step mechanism involving the initial proton transfer from  $O3'$  to D490, followed by the nucleophilic attack of  $O3'$  on the alpha phosphate of the incoming nucleotide. The energy barrier associated with the reaction is  $\sim 2$  kcal/mol smaller for the  $Mn^{2+}$  catalyzed reaction than for  $Mg^{2+}$ , in agreement with experiment.

Further insights into the reaction were provided by investigating the impact of individual residues on the critical points along the reaction path. To this end, the non-bonded interaction energy between each residue in the protein and the active site can be analyzed by means of an energy decomposition analysis (EDA). This analysis provides a qualitative assessment of the role of each amino acid on the reaction and can be used to compare to available mutagenesis experiments, or to predict possible mutation sites for subsequent experimental analysis. The residues found to be important for catalysis in Pol  $\lambda$  are shown in Figure 2.<sup>56</sup> None of the predicted residues had been experimentally investigated in Pol  $\lambda$  prior to our simulations. Only three homologous residues had been mutated experimentally in Pol  $\beta$ , and all exhibited impact on catalysis. Following our computational simulations, mutations on Pol  $\lambda$  were performed on R386<sup>59</sup> and K427,<sup>60</sup> which confirmed the role of these residues on activity and stabilization of the DNA substrate. These residues located in the so-called second shell around the active site also gave rise to the analysis of cancer SNPs as described in subsection 6.

*E. coli* DNA polymerase III (Pol III) is a complex that is relatively large composed of 10 subunits with multiple functions including DNA replication, post-replicative repair, and exonucleolytic proofreading.<sup>61,62</sup> We have investigated the  $\epsilon$  subunit in particular and its function as an exonuclease.<sup>63</sup> The  $\epsilon$  subunit (termed  $\epsilon$  in the subsequent discussion) preferentially removes incorrectly paired nucleotides and is a crucial component of DNA Pol III's high rate of fidelity.<sup>64,65</sup>

One metal and two metal mechanisms have been proposed<sup>66</sup> for the proofreading mechanism; our theoretical work focused

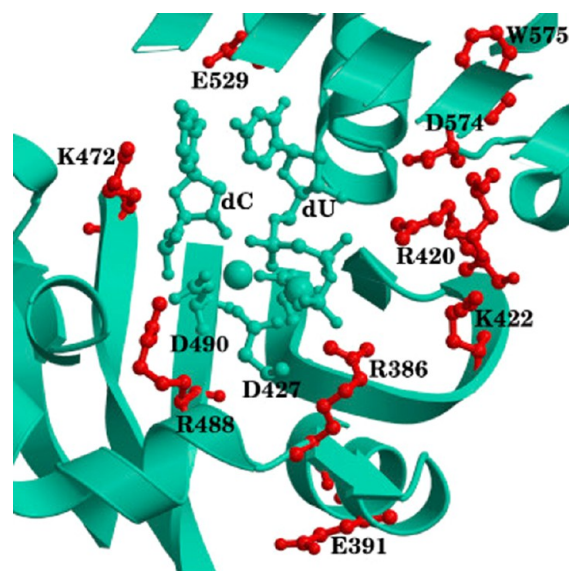


**Figure 2.** Catalytically relevant residues in Pol  $\lambda$ . Residues colored in red have large energetic contributions to transition state stability or are present in all transition states, residues in green correspond to the QM subsystem. Reprinted from Cisneros, G. A., Perera, L., García-Díaz, M., Bebenek, K., Kunkel, T. A., and Pedersen, L. G. (2008) Catalytic mechanism of human DNA polymerase  $\lambda$  with  $Mg^{2+}$  and  $Mn^{2+}$  from ab initio quantum mechanical/molecular mechanical studies. In *DNA Repair*, Vol. 7, pp 1824–1834, Copyright 2008, with permission from Elsevier.<sup>56</sup>

on the two-metal mechanism.<sup>67</sup> Additionally, the reaction catalyzed by  $\epsilon$  *in vivo* has been reported to be faster with  $Mn^{2+}$  than with  $Mg^{2+}$ , so the mechanisms for both of these metals were explored.<sup>66</sup> In both cases, the two metal mechanism involves a nucleophilic attack on the base to be excised by an attacking hydroxide ion; essentially, the reverse of the standard polymerase addition reaction. The formation of this ion is facilitated by the catalytic metal,  $Me_1$ , as seen in Figure 3.

The  $\epsilon$  subunit can associate with an additional  $\theta$  subunit, which has been proposed to promote its activity.<sup>68</sup> The  $\theta$  subunit also has a smaller homologue from bacteriophage P1,

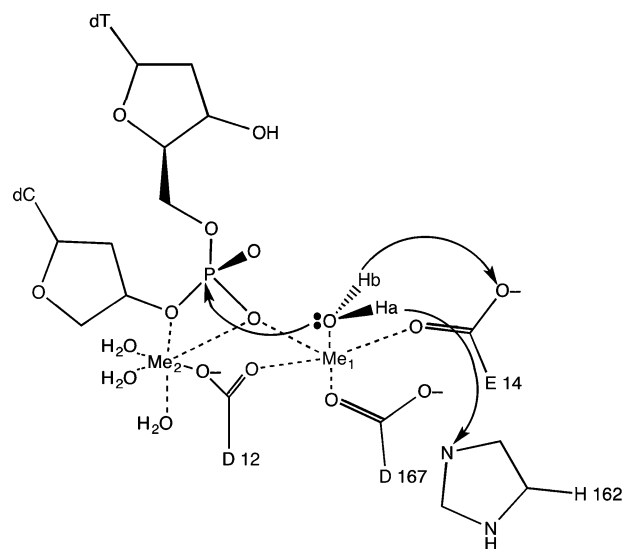


**Figure 3.** Reaction mechanism for the  $\epsilon$  subunit of DNA polymerase III holoenzyme.



HOT, which can also stabilize  $\epsilon$  and perform a similar function.<sup>69</sup> Crystal structures of the  $\epsilon$ -HOT complex with two metals in the active site were used to explore the mechanism using QM/MM and similar techniques as described for Pol $\lambda$ . Our simulations involved three different systems including the  $\epsilon$ -HOT complex with Mg<sup>2+</sup> or Mn<sup>2+</sup>, and free- $\epsilon$  with Mg<sup>2+</sup>. The calculated energy barriers suggest that  $\epsilon$  is slightly more active with Mn<sup>2+</sup> than with Mg<sup>2+</sup>; the  $\epsilon$ -HOT complex shows a slightly lower activation barrier compared with free- $\epsilon$  consistent with experiment.

A particularly interesting aspect of this study involves the number of ligands coordinated to the catalytic metal in the active site. The reported crystal structure for  $\epsilon$ -HOT, pdbid 2IDO, suggests that the catalytic metal is pentacoordinated.<sup>70</sup> This is an unusual coordination number, especially for Mg<sup>2+</sup>, which is considered to be the natural divalent cation for both DNA polymerases and exonucleases. Moreover, this pentacoordination is preferentially maintained along the reaction path according to our QM/MM simulations.<sup>67</sup> The more typical hexacoordination was also investigated but did not result in chemically reasonable structures for the catalytic step. This was observed for both Mn<sup>2+</sup>, which can maintain a pentacoordinated structure in the first coordination shell, and for Mg<sup>2+</sup>, for which it is less common but still present in other enzymes. This unusual coordination sphere has been subsequently reported in other enzymes.<sup>40,71,72</sup>

Additionally, we performed EDA in a similar manner to Pol $\lambda$  to determine residues that either stabilize or destabilize the TS for the proofreading mechanism (Figure 4).<sup>67</sup> Several residues near the active site and on HOT were shown to have a significant effects on catalysis. Four of these residues had been

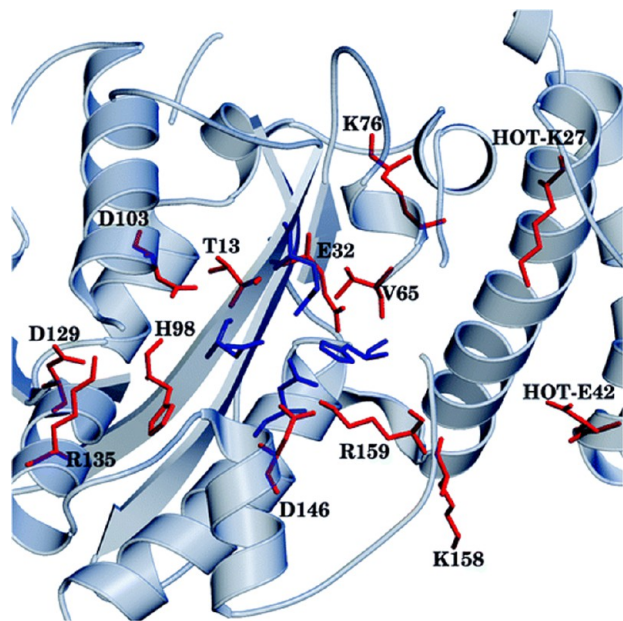


**Figure 4.** Catalytically important residues in  $\epsilon$ -HOT. Top: Residues colored in red have large energetic contributions to transition state stability and/or are present in all transition states, residues in blue are active site residues. Reproduced from Cisneros, G. A., Perera, L., Schaaper, R. M., Pedersen, L. C., London, R. E., Pedersen, L. G., and Darden, T. A. (2009) Reaction Mechanism of the  $\epsilon$  Subunit of *E. coli* DNA Polymerase III: Insights into Active Site Metal Coordination and Catalytically Significant Residues. *J. Am. Chem. Soc.* 131, 1550–1556. Copyright 2009 American Chemical Society.<sup>67</sup>

studied experimentally previously. All four showed mutator effects proportional to their (de)stabilization energies, with D103 and D129 showing particularly strong mutagenic effects.

We have also developed several methods to improve simulation accuracy and enable deeper analyses. One of these involves the combination of two quantum interpretative techniques, electron localization function (ELF) and non-covalent interaction (NCI) analysis, to investigate covalent and non-covalent regions. This combination was originally developed to investigate organic reactions in gas phase<sup>73</sup> and subsequently extended by us to enzymatic reaction mechanisms.<sup>34</sup> We applied ELF/NCI analysis to further examine the role of the electronic structure on the intermolecular interactions and metal coordinations related to the reactions catalyzed by Pol $\lambda$  and  $\epsilon$ . For Pol $\lambda$ , the ELF/NCI analysis revealed that the interaction between O3' on the primer and Mg<sup>2+</sup> was weaker than for Mn<sup>2+</sup>, as indicated by the associated NCI surface. Concomitantly, the interaction between O3' and the phosphate oxygen coordinated to the metal ions was stronger for Mg<sup>2+</sup> than for Mn<sup>2+</sup> (Figure 5). These results are consistent with our previous QM/MM (and experimental) results where the barrier for proton transfer is higher for Mg<sup>2+</sup>;<sup>63</sup> further details about the ELF results can be seen in Subsection 3.

Similarly, for the  $\epsilon$  subunit of Pol III, the Mn<sup>2+</sup> ion shows electronic density splitting in the surfaces associated with the metal ions. This splitting is not present for Mg<sup>2+</sup>, indicating that the Mn<sup>2+</sup> ion has stronger interactions with pertinent residues in the active site as compared to Mg<sup>2+</sup>. Interestingly, the catalytic metal exhibits five splitting basins as shown in Figure 6, which is also consistent with the pentacoordination of Me1 as explained above. Further insights into metal mutagenicity using ELF/NCI are discussed below in section 3.

**2.1. Third Metal in Pol $\lambda$  Mechanism.** As explained above, the synthesis of DNA by DNA polymerases involves a general two metal ion mechanism. Recently, Nakamura et al. reported the existence of a transient third metal ion in the *in crystallo* reaction of Pol $\mu$  based on time-resolved X-ray crystallography.<sup>74</sup> Wilson and co-workers have published similar evidence for Pol $\beta$ .<sup>75</sup> On the basis of these results, Perera et al. have performed extensive computational simulations to investigate the role of this third cation in the reaction mechanism of Pol $\beta$ .<sup>27,41</sup> Their results suggest that this third metal does not affect the forward chemical step (DNA synthesis) and significantly impairs the pyrophosphorolysis (backward) reaction.

Pol $\lambda$  is 35% identical to Pol $\beta$  and thus the question arises of whether this transient third metal is also present in the Pol $\lambda$  reaction. We have explored the possible role of the third metal ion in Pol $\lambda$  using our own QM/MM program, LICHEM.<sup>76</sup> As reported in ref 74, the comparison of the calculated energies of Pol $\lambda$  reactant and product structures with a third metal included in the active site results in a stabilization of the product relative to the reactant (Figure 7). This is in contrast to our original reported path for the mechanism of Pol $\lambda$ , where the calculated reaction energy is endoergic by around 4–5 kcal/mol. Thus, our initial calculations are consistent with the work of Perera et al. and Genna et al. in that the third metal stabilizes the product structure and thus reduces the likelihood of the backward reaction.<sup>27,77</sup> In addition, the resulting distances for the active site in the optimized structures in Pol $\lambda$  are similar to those reported by Perera et al., with the third metal

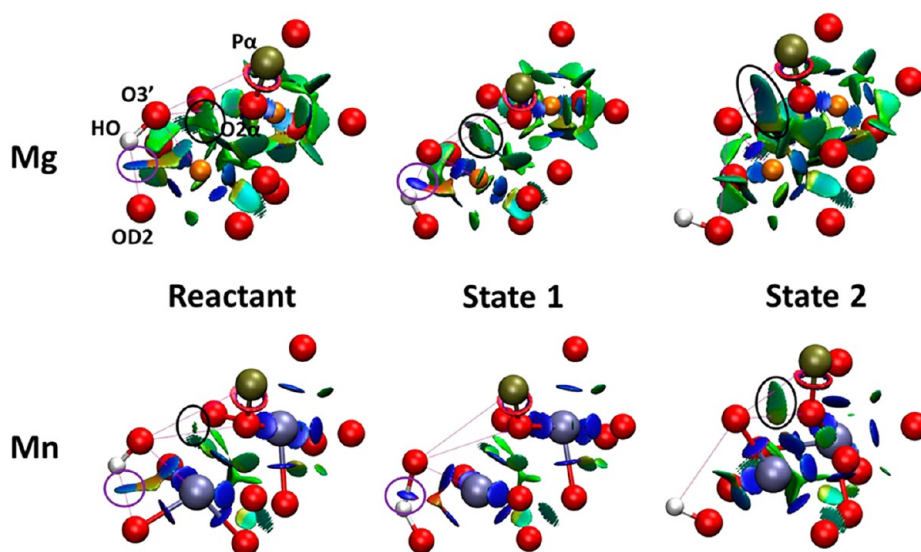


**Figure 5.** NCIplot for Pol  $\lambda$  reactant structures, with strong attractive forces denoted in blue, strong repulsive forces denoted in red, and weak forces denoted in green. Reproduced from Fang, D., Chaudret, R., Piquemal, J.-P., and Cisneros, G. A. (2013) Toward a Deeper Understanding of Enzyme Reactions Using the Coupled ELF/NCI Analysis: Application to DNA Repair Enzymes. *J. Chem. Theo. Comp.* 9, 2156–2160. Copyright 2013 American Chemical Society.<sup>54</sup>

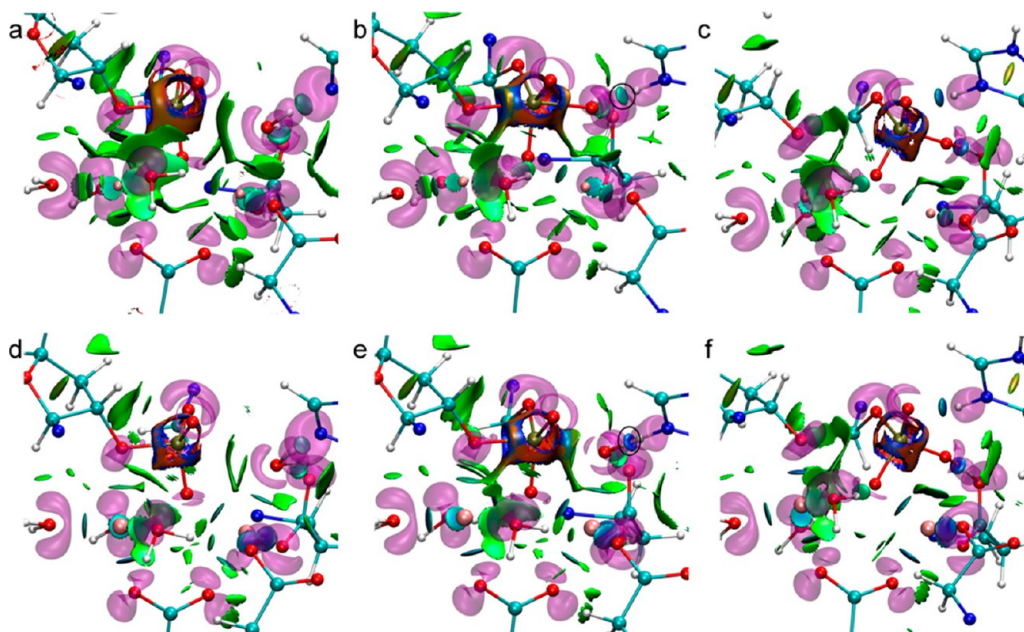


**Figure 6.** Combined NCI and ELF surfaces for the  $\epsilon$  subunit of Pol III. ELF surfaces are shown in transparent purple, and NCI surfaces shown as solid red/green/blue surfaces. Panels a–c show the reactant, transition state and product structures for  $Mg^{2+}$ , while panels d–f show the same for  $Mn^{2+}$ . Reproduced from Fang, D., Chaudret, R., Piquemal, J.-P., and Cisneros, G. A. (2013) Toward a Deeper Understanding of Enzyme Reactions Using the Coupled ELF/NCI Analysis: Application to DNA Repair Enzymes. *J. Chem. Theo. Comp.* 9, 2156–2160. Copyright 2013 American Chemical Society.<sup>54</sup>

coordinating to the apical oxygen on  $P\alpha$  with distances around 2.1 Å for reactant and product.

### 3. METAL MUTAGENICITY IN DNA POLYMERASES

The requirement of metal cations to facilitate the reaction in DNA Pols gives rise to the possibility of replacement of the "natural" cation,  $Mg^{2+}$ , by other metals. It is known that several cations are carcinogenic or genotoxic, and these effects are due to the inhibition of DNA repair transactions.<sup>78</sup> Indeed, the replacement of  $Mg^{2+}$  ions in the active site of DNA polymerases by metals such as Cr(II), Cd(II), Ni(II), Ca(II),

Na(+), or Mn(II) results in either a decrease in synthesis fidelity or outright inhibition.<sup>57</sup> Pelletier et al. investigated the effect of different metals in ternary structures of DNA Pol $\beta$ .<sup>79</sup> Their results show that metals other than  $Mg^{2+}$  result in changes in the active site geometry.

On the basis of our previous results on the reaction mechanism of Pol $\lambda$ , we investigated the effect of nine different cations including  $Mg^{2+}$ ,  $Na^+$ ,  $Ca^{2+}$ ,  $Zn^{2+}$ ,  $Co^{2+}$ ,  $Cr^{2+}$ ,  $Cu^{2+}$ ,  $Mn^{2+}$ , and  $Ni^{2+}$  using QM/MM methods.<sup>80</sup> In addition to the structural effects, we performed electron localization function



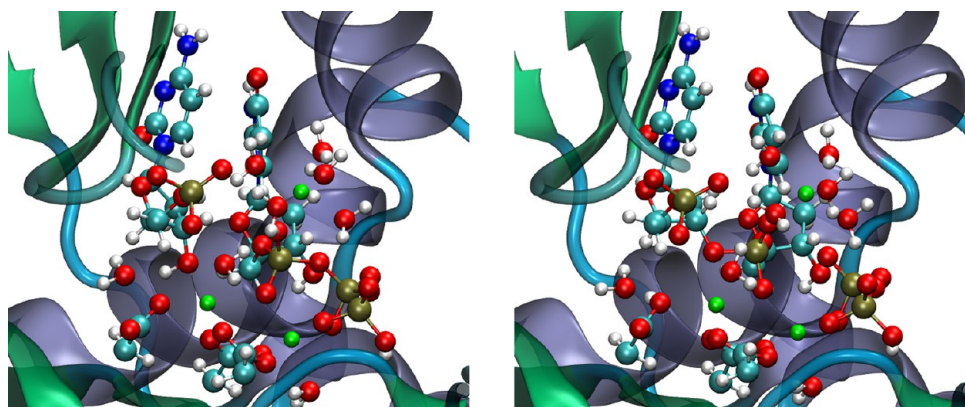


**Figure 7.** Close-up of the active site for the optimized reactant (left) and product (right) structures of Pol $\lambda$  with the third metal in the active site.

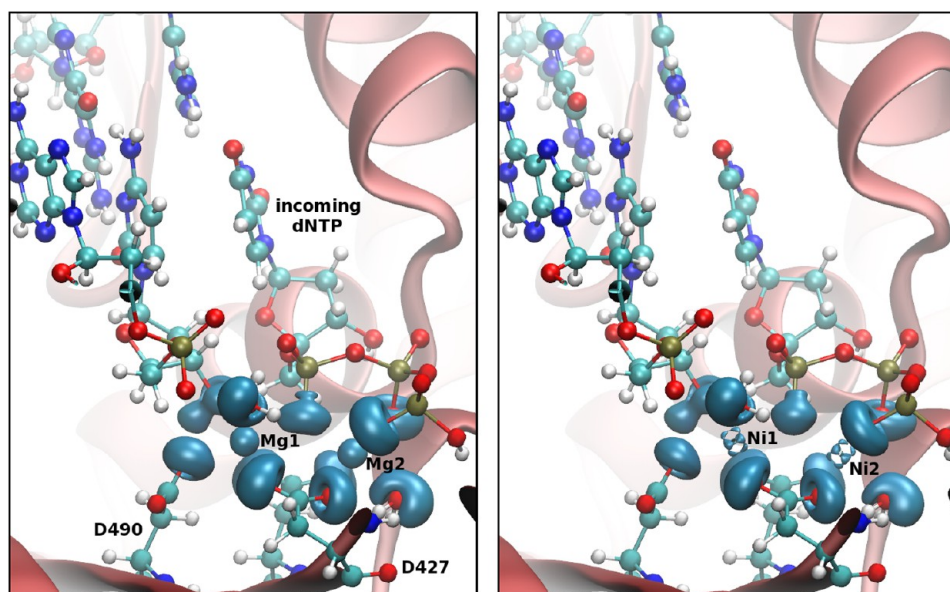


**Figure 8.** ELF analysis for the active site of Pol $\lambda$  with Mg $^{2+}$  (left) and Ni $^{2+}$  (right) occupying the catalytic and nucleotide binding metal sites. Reproduced from Chaudret, R., Piquemal, J.-P., and Cisneros, G. A. (2011) Correlation between electron localization and metal ion mutagenicity in DNA synthesis from QM/MM calculations. *Phys. Chem. Chem. Phys.* 13, 11239–11247, with permission from the PCCP Owner Societies.<sup>80</sup>

(ELF) analyses on all the resulting systems to gain insights into the effects of the metals on the electronic structure.

The structures obtained from our simulations indicate that the overall arrangement of the active site is largely unaltered regardless of the cation, with only subtle differences arising such as very slight increases of 0.2–0.4 Å between the metals and the atoms in the first coordination shell. Similarly, the nucleophilic attack distance (O3' to P $\alpha$ ) increases slightly,  $\sim$ 0.3 Å, for two of the three inhibitor cations, Na $^{+}$  and Ca $^{2+}$ .

To further understand the differences between these systems given the very slight changes in geometry, we turned to the analysis of the electronic structure via ELF. The results from the ELF analysis are striking in that out of the nine tested cations, significant differences were observed between the calculated systems with inhibitor and mutagenic cations compared to the Mg $^{2+}$  system.<sup>80</sup> In particular, the ELF analysis indicates that when two Mg $^{2+}$  occupy the active site, the cations and incoming nucleotide experience a particular electronic polarization. By contrast, the inhibitory (Ca $^{+}$ , Na $^{+}$ , and Zn $^{2+}$ ) and mutagenic (Co $^{2+}$ , Cr $^{2+}$ , Cu $^{2+}$ , Mn $^{2+}$ , and Ni $^{2+}$ ) cations exert a different (hyper)polarization on the oxygen atoms on the triphosphate of the incoming nucleotide. In addition, the

enzyme environment also significantly affects the metals in that only the Mg $^{2+}$  shows a single basin around the metals, whereas all other metals are (hyper-)polarized in such a way that the metal exhibits multiple basins (Figure 8).

Thus, the detailed analysis of the electronic structure of Pol $\lambda$  suggests that the replacement of the natural metals by other cations results in a change in polarization that may be responsible for the observed inhibitory or mutagenic effects of the replacing cations depending on their identity.<sup>80</sup>

#### 4. DNA SYNTHESIS FIDELITY CHECKING

The accurate replication of the genomic data is crucial for organismal survival. DNA polymerases are arguably some of the most important enzymes in the transactions involved in replication. For example, the replication error rates in *E. coli* are around 1 in 10 $^{10}$ .<sup>64</sup> This very low error rate (high fidelity) is due to at least three steps that are involved in the replication of DNA: (1) base selection, (2) proofreading, and (3) mismatch repair. DNA Pol I is a key player in the achievement of the low error rates due to its participation in two of the three steps via three enzymatic activities: DNA polymerase, 5'  $\rightarrow$  3' exonuclease, and 3'  $\rightarrow$  5' exonuclease.<sup>81</sup>

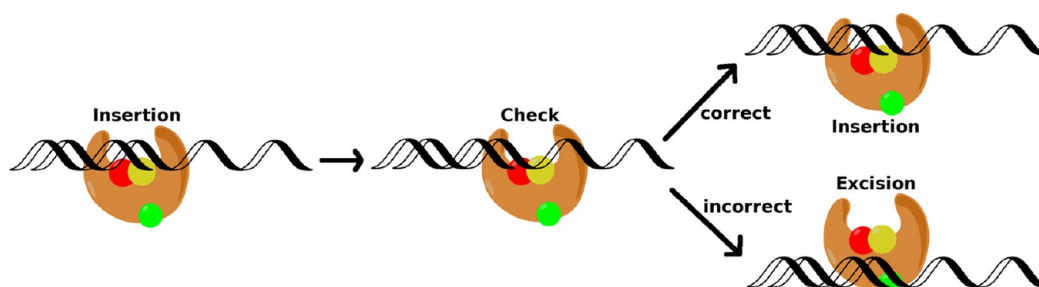


**Figure 9.** Schematic diagram of the proposed fidelity checking process in DNA polymerase I. Following nucleotide insertion, the DNA is translocated to the checking site. If the inserted base pair is a correct pair, the polymerase continues. If not, the DNA is shifted to the exonuclease domain and the incorrect base pair is excised. Reproduced from Graham, S.E., Syeda, F., and Cisneros, G. A. (2012) Computational Prediction of Residues Involved in Fidelity Checking for DNA Synthesis in DNA Polymerase I. *Biochemistry* 51, 2569–2578. Copyright 2012 American Chemical Society.<sup>93</sup>

The Klenow fragment (KF) is a functional fragment of the *POLA* gene, which codes for PolI, and contains the polymerase and 3' → 5' exonuclease activities.<sup>82–91</sup> The KF has provided a very useful system to learn a great deal about DNA polymerases including reasons for nucleotide misinsertion discrimination and decrease in synthesis fidelity rates, among other insights.<sup>84,91</sup> The KF is a member of the A family of polymerases, which includes various other highly studied polymerases such as DNA PolI from *Thermus aquaticus*, KlenTaq fragment, and *Bacillus stearothermophilus* [Bacillus fragment (BF)].

The discrimination of correct versus incorrect nucleotide insertion in KF has been investigated with single-molecule Förster resonance energy transfer (FRET) by Christian et al.<sup>92</sup> The single-molecule results indicated a movement along the DNA following synthesis that had not been previously observed. The authors proposed that KF translocates two bases downstream along the DNA strand following a nucleotide incorporation before backtracking for the next round of incorporation (Figure 9).<sup>92</sup> On the basis of these results, Christian et al. proposed a possible post-insertion fidelity checking site to check that the newly incorporated base is not mismatched with the templating base. The checking site is assumed to be located immediately behind the pre-insertion site ( $n - 1$  position along the DNA)

We employed various computational techniques to investigate the location of potential residues that could be involved in the putative checking site on KF, BF, and KlenTaq.<sup>93,94</sup> MD simulations were performed on all three polymerases containing correctly or incorrectly paired bases with either a blunt end (KF, BF)<sup>93</sup> or a two-base overhang template (KlenTaq).<sup>94</sup> The resulting ensembles were subjected to various analyses including energy decomposition (EDA), electrostatic free energy response (EFER),<sup>95,96</sup> and non-covalent interaction (NCI)<sup>97,98</sup> to investigate whether/if any residues show changes in interaction with correctly or incorrectly paired bases.

The interaction analyses revealed that there are a number of residues around the putative checking site (Figure 10). Correlation of EDA, EFER, and NCI analyses for all three systems (KF, BF, and KlenTaq) suggests that there are six residues with altered interactions with mismatched bases compared to correctly paired bases in the putative checking site. Figure 11 shows a condensed sequence alignment for A family polymerases that indicates the six residues with altered interactions.

Various residues that show altered interactions from our computational analysis have been reported to result in changes to DNA fidelity synthesis in KF and KlenTaq. In particular,

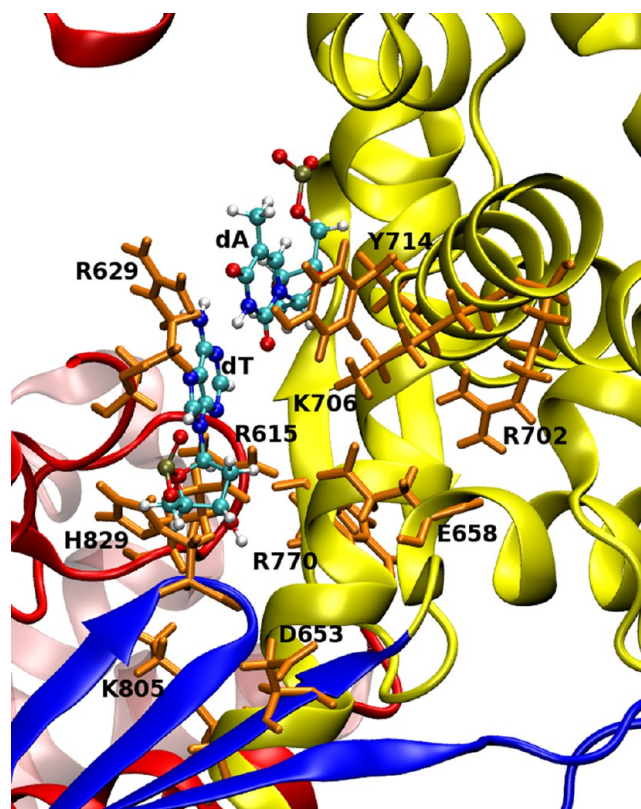


**Figure 10.** Positions of residues with altered interactions in KF and BF (orange sticks). The structure and numbering correspond to BF. Polymerase subdomains are colored red, blue, yellow, and mauve for the palm, fingers, thumb, and exonuclease, respectively. DNA bases (T:A) in the preinsertion site are shown as balls and sticks. Reproduced from Graham, S.E., Syeda, F., and Cisneros, G. A. (2012) Computational Prediction of Residues Involved in Fidelity Checking for DNA Synthesis in DNA Polymerase I. *Biochemistry* 51, 2569–2578. Copyright 2012 American Chemical Society.<sup>93</sup>

residues R668 and R682 in KF (R615, R629 in BF and R573, R587 in KlenTaq) have been reported to be important in the partitioning of the DNA primer terminus between the polymerase and exonuclease active sites as well as mispair discrimination for synthesis fidelity.<sup>88,89</sup> The correlation between experimental mutagenesis studies indicating the role of these residues in fidelity and the possible involvement of these residues in the fidelity-checking step provide possible targets for further investigation of this intriguing hypothesis.



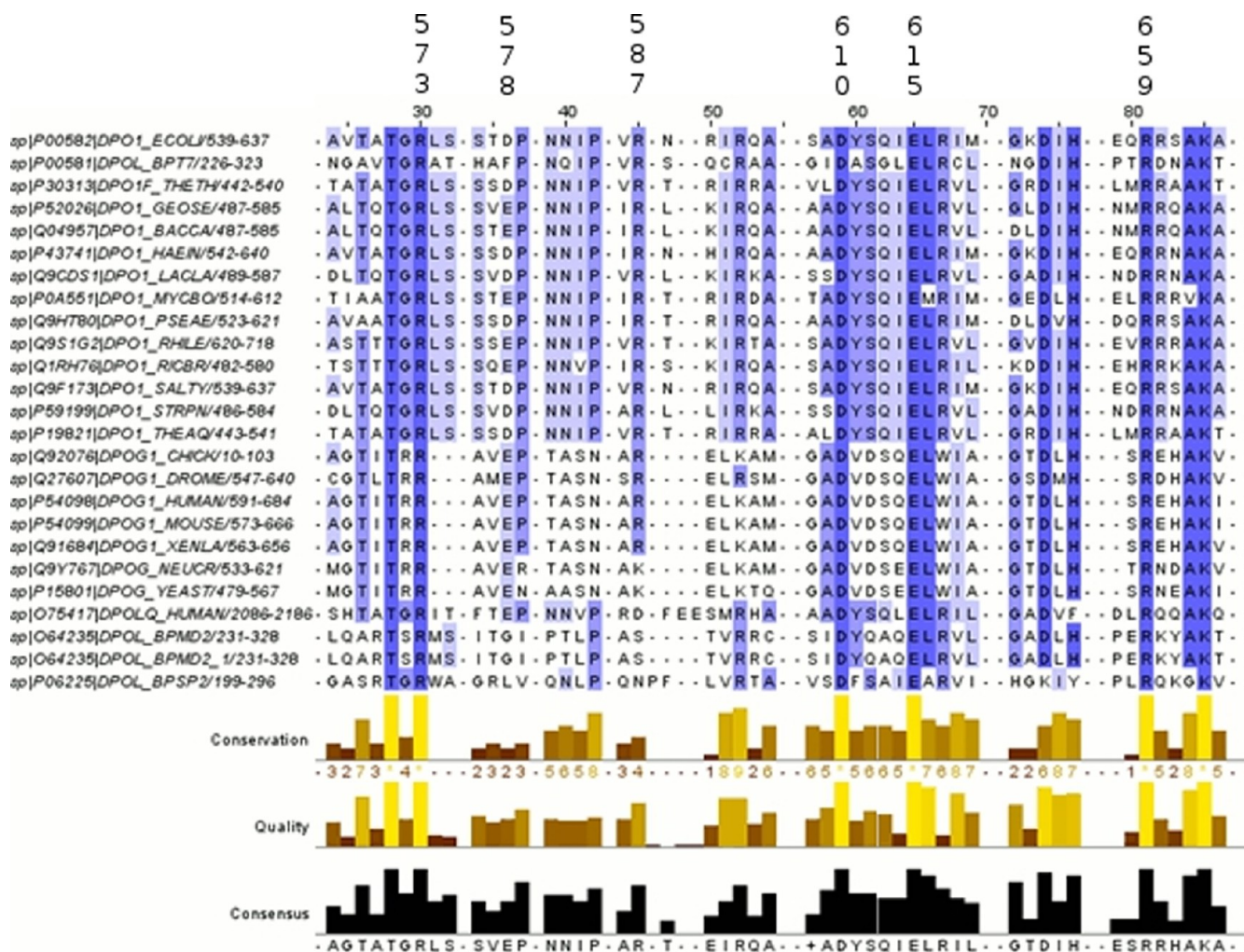


**Figure 11.** Condensed alignment for family A DNA polymerases with the common residues with altered interactions in the putative  $(n - 1)$  checking site indicated. The numbering corresponds to Klentaq. Reproduced from Elias, A. A., and Cisneros, G. A. (2014) Computational Study of Putative Residues Involved in DNA Synthesis Fidelity Checking in *Thermus aquaticus* DNA Polymerase I. In *Adv. Protein. Chem. Struct. Biol.* 96, 39–75, Copyright 2014, with permission from Elsevier.<sup>94</sup>

## 5. EFFECTS OF MUTAGENIC LESIONS ON STRUCTURE AND FUNCTION OF DNA POLYMERASE IV

Y-family polymerases, such as DNA polymerase IV (Dpo4), have large, flexible, and solvent exposed active sites that can accommodate bulky lesions, which is likely crucial to their ability to perform translesion synthesis (TLS). DNA can be damaged in a variety of ways, including the incorporation of endogenously produced molecules such as polycyclic aromatic hydrocarbons (PAHs).<sup>99</sup> Benzo[a]pyrene (B[a]P) is a particularly bulky adduct that can add to DNA in several conformations with different effects on DNA replication.<sup>5,100</sup>

We have recently carried out computational simulations to aid in the understanding of biochemical and single molecule FRET experiments for Dpo4 with B[a]P damage. The experimental results indicate that the cis conformation of B[a]P adducted to guanine exhibits two different behaviors depending on the solvent environment; in a pure water system, the adduct takes the place of the guanine residue, intercalated within the DNA helix, and replication does not proceed past that point.<sup>101</sup> In a 10% dimethyl sulfoxide (DMSO)/90% water mixture, two different FRET states are observed and Dpo4 is able to continue the DNA synthesis (TLS). Additionally, a G-G

mismatch is more stable than the correct G-C base pairing, resulting in increased errors in TLS.

We performed classical MD simulations on Dpo4 with B[a]P incorporated to the DNA in pure water and in the water/DMSO mixture.<sup>101</sup> Our results indicate that the B[a]P indeed intercalates with the DNA and does not allow the adduct to be everted from the double strand when in pure water. Conversely, in the water/DMSO mixture, the B[a]P adduct flips out into an open space next to the active site underneath the finger domain in a solvent exposed conformation, allowing replication to continue (Figure 12). This is enabled by DMSO reducing the dielectric constant of the solvent around the B[a]P adduct (effectively microsolvating the B[a]P) and allowing it to be everted from the double helix and thus avoiding the arrest of the polymerase.

## 6. DISCOVERY AND CHARACTERIZATION OF CANCER MUTANTS ON DNA POLS

The discovery of various residues involved in catalysis in the “2nd-shell” of Pol $\lambda$  (Figure 2) raised a question about how many of these residues are conserved among all human polymerases. A detailed sequence–structure alignment reveals that five of the nine catalytically relevant second-shell residues



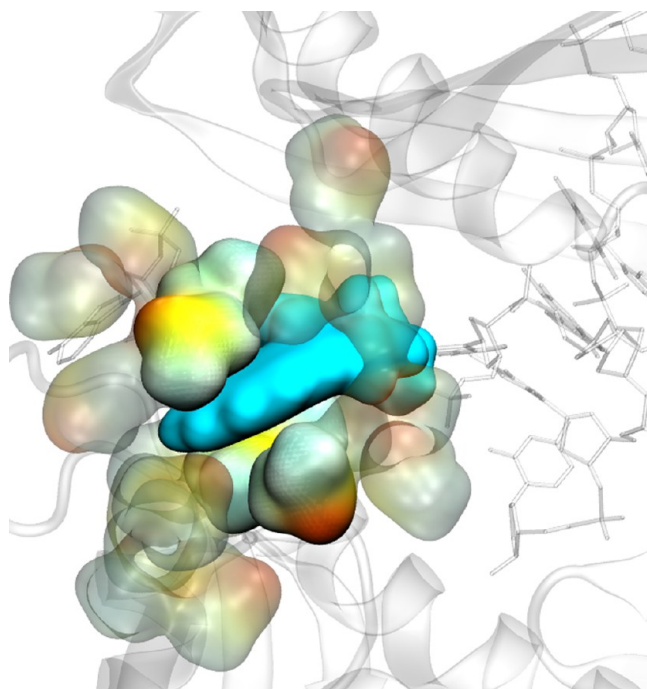


**Figure 12.** Microsolvation of the flipped out conformation of cis-benzo[a]pyrene (blue surface) with dimethyl sulfoxide (yellow and green surfaces).

are at least partially conserved (Figure 13). This points to the evolutionary importance of these residues for polymerase activity and/or function.

Pol	Residue				
$\lambda$	R386	S417	R420	K472	R488
$\beta$	R149	S180	R183	K234	R254
$\mu$	-	-	R323	R387	R416
$\sigma$	-	S36	-	K80	R174
TdT	-	-	R336	K402	R431
$\theta$	R1551	-	R662	H1711	K1743
$\Upsilon$	R493	-	H932	H1134	R1234
$\delta$	K671	S605	R667	K807	-
$\epsilon$	K769	-	R765	K954	-
$\alpha$	K936	S863	R931	K1053	-
$\zeta$	K2701	S2617	R2697	K2833	-
$\eta$	K231	-	R55	-	K224
$\iota$	K214	-	R71	-	K207
$\kappa$	R328	-	R144	-	K321

**Figure 13.** Second-shell residues conserved among 14 different human polymerases.

On the basis of these results, we wondered if there are any natural variants associated with a disease state that result in mutations of these second-shell residues and how these may affect the structure and function. Several polymerases have been linked specifically to cancer, such as Pol $\eta$ , which has a well-documented relationship with skin cancer.<sup>3,102,103</sup> To this end, we developed a methodology that combines a targeted search for single nucleotide polymorphisms (SNPs) on selected genes, statistical validation of the uncovered SNPs, and computational simulations of the wild-type and SNP variants to determine if/

whether the disease variant shows a difference in its structure or function. The search algorithm was implemented in a computer program called Hypothesis Driven-SNP-Search, or HyDn-SNP-S.<sup>104</sup>

The first application of HyDn-SNP-S was performed to uncover SNPs on all DNA polymerase genes for four different genome-wide association studies comprising melanoma, lung, prostate, and breast cancer (Figure 14). Following logistical

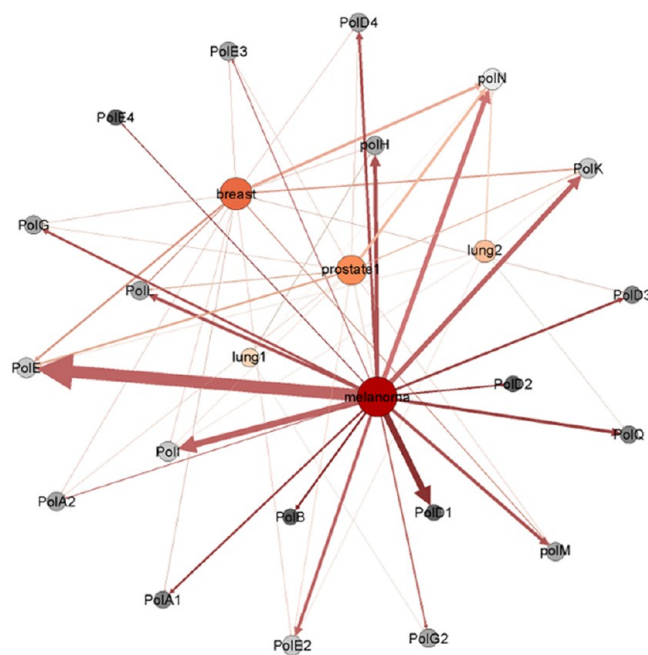


**Figure 14.** Edge-node network of the HyDn-SNPs results for DNA polymerases. Phenotypes and polymerases are shown as nodes, edges are weighted by total number of SNPs connecting each phenotype to each polymerase. Reproduced from Swett, R. J., Elias, A., Miller, J. A., Dyson, G. E., and Cisneros, G. A. (2013) Hypothesis driven single nucleotide polymorphism search (HyDnSNP-S). In *DNA Repair 12*, 733–740, Copyright 2013, with permission from Elsevier.<sup>104</sup>

regression, 79 exonic non-synonymous SNPs were found to be statistically significantly associated with disease status.<sup>104</sup> Further analysis to determine derived haplotypes of the uncovered SNPs with the selected cancer phenotypes resulted in two new haplotypes for breast and prostate cancer. The first haplotype is composed of two SNPs on *POLL*, rs3730477 and rs3730463, and results in a three-fold increase in risk of breast cancer. The second haplotype is constructed from three SNPs on *POLG*, rs3087374, rs2351000, and rs2247233. The resulting haplotype indicates having two copies of the G–C–A haplotype ( $p = 0.008$ ) results in a 9.64-fold increase in prostate cancer disease status.<sup>104</sup>

In addition to uncovering a large number of previously unknown cancer missense SNPs on DNA polymerases, we performed computational simulations on one particular SNP. One of the SNPs on Pol $\lambda$ , rs3730477, is associated with breast cancer status and results in the R438W variant. R438 is located around 12 Å away from the active site (Figure 15). This residue sits at the end of loop1, which is crucial for Pol $\lambda$  fidelity, and the SNP variant has been shown to give rise to chromosomal abnormalities.<sup>105,106</sup> We performed MD simulations on the binary and ternary structures of wild-type and the R438W variant to determine the possible impact of the breast-cancer mutation on the structure or function of Pol $\lambda$ . Our MD

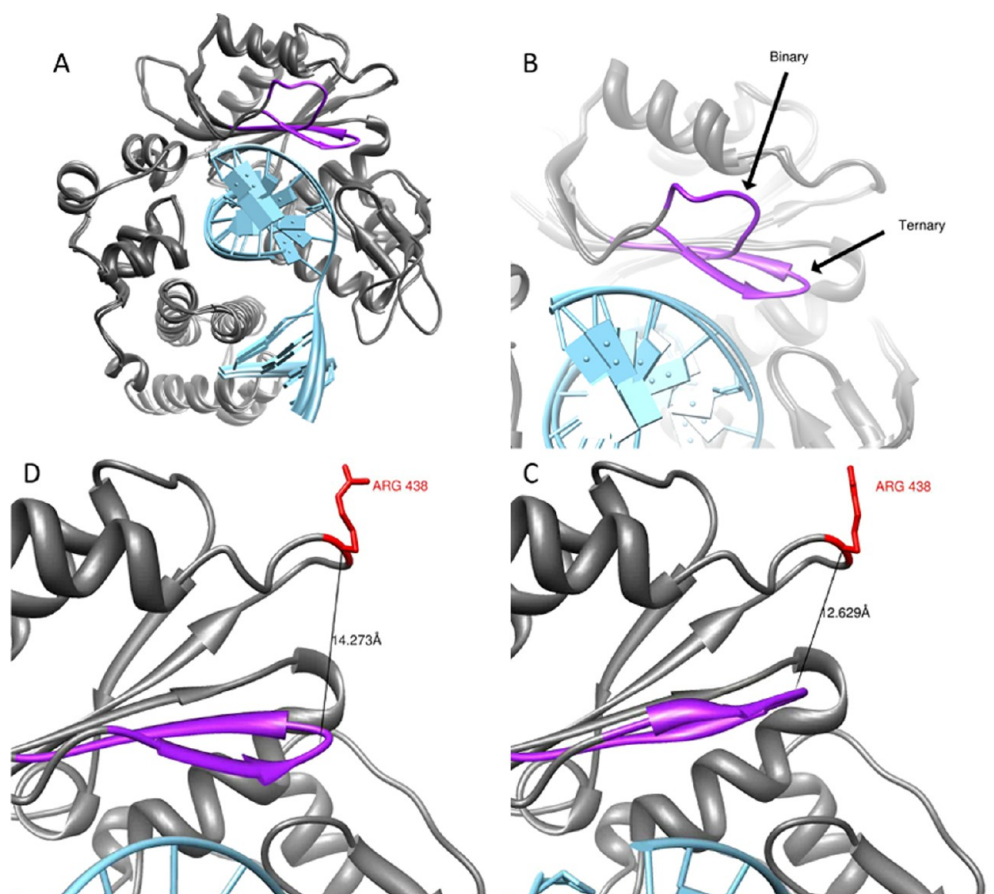


**Figure 15.** (A) Overlay of Pol $\lambda$  in the binary and ternary conformations. DNA is shown in light blue, and Loop 1 is shown in purple. (B) Differences in Loop 1 orientation between the two conformations. Distance between position 438 and Loop 1 following an interpolation between the two structures at its (D) furthest and (C) closest approaches. Reproduced from Swett, R. J., Elias, A., Miller, J. A., Dyson, G. E., and Cisneros, G. A. (2013) Hypothesis driven single nucleotide polymorphism search (HyDnSNP-S). In *DNA Repair* 12, 733–740, Copyright 2013, with permission from Elsevier.<sup>104</sup>

simulations indicate that the mutation of R by W at position 438 results in a change in the dynamics of loop 1, without affecting the overall motions of the rest of the protein. Our results suggest that the alteration of the motion of loop 1, which is experimentally known to be crucial for fidelity, could affect the function of this critical structural feature and help explain the observed decrease in fidelity.<sup>104</sup> Recently, on the basis of our work, Sweasy and co-workers have confirmed that rs3730477 can be used as a biomarker for breast cancer, and, more importantly for individuals with this particular mutation, estrogen treatment may increase the risk of breast cancer status.<sup>107</sup>

## 7. SUMMARY AND PERSPECTIVE

Computational simulations of DNA polymerases using classical, quantum mechanical, and hybrid QM/MM methods have enabled a deeper understanding of a variety of facets related to their structure, function, and mechanism. Detailed analysis at the atomic and electronic structure level enabled by these methods has been shown to be useful to gain insights into factors of metal mutagenicity, nucleotide discrimination, and impact of protein residues on catalytic activity. The application of novel bioinformatic techniques to uncover cancer-associated SNPs in DNA polymerases has resulted in a large number of statistically significantly associated biomarkers on DNA polymerases for four distinct cancer phenotypes. The use of

computational simulations on these cancer mutants has provided possible explanations for the impact of these cancer mutations on the function of the proteins.

In the future, it is expected that the improvement of simulation methods, including more accurate classical potentials, coupled with better levels of QM theory, enabled by larger computing capacity will provide more opportunities for deeper insights into these systems. For example, longer simulation times will enable the possibility to study the transfer of ssDNA from the polymerase to the exonuclease to investigate steps required for proofreading. Continuing the use of computational simulations to investigate the impact of cancer-associated SNPs on DNA polymerase structure, function, and dynamics will provide the possibility to investigate the effect of these cancer mutations at an atomic level. It is clear that the use of computational simulations of DNA polymerases is a robust and well-established field that has provided important contributions and will continue to aid in the detailed understanding of these important enzymes.

## ■ AUTHOR INFORMATION

### Corresponding Author

\*E-mail: [andres@unt.edu](mailto:andres@unt.edu). Phone: 940-565-4296.

### ORCID

Alice R. Walker: 0000-0002-8617-3425

G. Andrés Cisneros: 0000-0001-6629-3430



## Funding

This work was supported by the National Institutes of Health—NIGMS, Grant Nos. R01GM108583, R01GM118501 to G.A.C., and by the NVIDIA Foundation Compute the Cure program.

## Notes

The authors declare no competing financial interest.

## Biographies

**Alice R. Walker** obtained her B.Sc. in Chemistry from the University of Michigan-Dearborn and is currently a Ph.D. candidate at the University of North Texas under Dr. G. Andrés Cisneros. Her research interests are centered around various aspects of computational biochemistry, particularly modifying and applying quantum mechanical/molecular mechanics to biochemical systems associated with cancer and disease.

**G. Andrés Cisneros** received a B.Sc. in Chemistry from the National Autonomous University of Mexico (UNAM) and a Ph.D. in Chemistry from Duke University. Afterward, he worked as an intramural postdoctoral fellow in the National Institute of Environmental Health Sciences/NIH. He is currently an Associate Professor in the Department of Chemistry at the University of North Texas and a member of CASCaM at UNT. His research interests include the study of DNA replication/repair systems, development, and application of accurate methods for chemical/biochemical simulations with emphasis on force field and QM/MM development and simulation of ionic liquid systems.

## ACKNOWLEDGMENTS

Resources from the National Institutes of Health—NIGMS, the NVIDIA Foundation Compute the Cure program, and computing time from Wayne State's C&IT and UNT's CASCaM are gratefully acknowledged.

## ABBREVIATIONS

Pol, polymerase; BER, base excision repair; NHEJ, non-homologous end joining; MD, molecular dynamics; QM, quantum mechanics; QM/MM, quantum mechanics/molecular mechanics; P $\alpha$ , alpha phosphate; PPi, pyrophosphate; EDA, energy decomposition analysis; SNP, single nucleotide polymorphism; HOT, homologue of theta; TS, transition state; ELF, electron localization function; NCI, noncovalent interaction; KF, Klenow fragment; FRET, Förster resonance energy transfer; EFER, electrostatic free energy response; Dpo4, DNA polymerase IV; TLS, translesion synthesis; PAH, polycyclic aromatic hydrocarbon; DMSO, dimethyl sulfoxide; B[a]P, benzo[a]pyrene

## REFERENCES

- (1) Starcevic, D., Dalal, S., and Sweasy, J. B. (2004) Is there a link between DNA polymerase  $\beta$  and cancer? *Chem. Commun.* 3, 98–1001.
- (2) Iwanaga, A., Ouchida, M., Miyazaki, K., Hori, K., and Mukai, T. (1999) Functional mutation of DNA polymerase  $\beta$  found in human gastric cancer - inability of the base excision repair in vivos. *Mutat. Res., DNA Repair* 435, 121–128.
- (3) Lange, S. S., Takata, K., and Wood, R. D. (2011) DNA polymerases and cancer. *Nat. Rev. Cancer* 11, 96–110.
- (4) Loeb, L. A., and Monnat, R. J. (2008) DNA polymerases and human disease. *Nat. Rev. Genet.* 9, 594–604.
- (5) Broyde, S., Wang, L., Rechkoblit, O., Geacintov, N. E., and Patel, D. J. (2008) Lesion processing: high-fidelity versus lesion-bypass DNA polymerases. *Trends Biochem. Sci.* 33, 209–219.

- (6) Mulholland, A. J., Roitberg, A. E., and Tuñón, I. (2012) Enzyme dynamics and catalysis in the mechanism of DNA polymerase. *Theor. Chem. Acc.* 131, 1286.

- (7) Johnson, K. A. (2010) The kinetic and chemical mechanism of high-fidelity DNA polymerases. *Biochim. Biophys. Acta, Proteins Proteomics* 1804, 1041–8.

- (8) Kunkel, T. A. (2003) Considering the cancer consequences of altered DNA polymerase function. *Cancer Cell* 3, 105–110.

- (9) Aravind, L., and Koonin, E. V. (1998) Phosphoesterase domains associated with DNA polymerases of diverse origins. *Nucleic Acids Res.* 26, 3746–52.

- (10) Gouge, J., Ralec, C., Henneke, G., and Delarue, M. (2012) Molecular recognition of canonical and deaminated bases by P. abyssi family B DNA polymerase. *J. Mol. Biol.* 423, 315–36.

- (11) Jozwiakowski, S. K., Keith, B. J., Gilroy, L., Doherty, A. J., and Connolly, B. A. (2014) An archaeal family-B DNA polymerase variant able to replicate past DNA damage: occurrence of replicative and translesion synthesis polymerases within the B family. *Nucleic Acids Res.* 42, 9949–9963.

- (12) Khare, V., and Eckert, K. A. (2002) The proofreading 3'→5' exonuclease activity of DNA polymerases: a kinetic barrier to translesion DNA synthesis. *Mutat. Res., Fundam. Mol. Mech. Mutagen.* 510, 45–54.

- (13) Yang, W. (2014) An Overview of Y-Family DNA Polymerases and a Case Study of Human DNA Polymerase  $\beta$ . *Biochemistry* 53, 2793–2803.

- (14) Bebenek, K., and Kunkel, T. A. (2004) Functions of DNA polymerases. *Adv. Protein Chem.* 69, 137–165.

- (15) Moon, A. F., García-Díaz, M., Batra, V. K., Beard, W. A., Bebenek, K., Kunkel, T. A., Wilson, S. H., and Pedersen, L. C. (2007) The X family portrait: Structural insights into biological functions of X family polymerases. *DNA Repair* 6, 1709–1725.

- (16) Federley, R. G., and Romano, L. J. (2010) DNA polymerase: structural homology, conformational dynamics, and the effects of carcinogenic DNA adducts. *J. Nucleic Acids* 2010, 1.

- (17) Rucker, R., Oelschlaeger, P., and Warshel, A. (2009) A binding free energy decomposition approach for accurate calculations of the fidelity of DNA polymerases. *Proteins: Struct., Funct., Genet.* 78, 671–680.

- (18) Shen, H., and Li, G. (2014) Bridging the Missing Link between Structure and Fidelity of the RNA-Dependent RNA Polymerase from Poliovirus through Free Energy Simulations. *J. Chem. Theory Comput.* 10, 5195–5205.

- (19) Florián, J., Goodman, M. F., and Warshel, A. (2003) Computer simulation studies of the fidelity of DNA polymerases. *Biopolymers* 68, 286–299.

- (20) Meli, M., Sustarsic, M., Craggs, T. D., Kapanidis, A. N., and Colombo, G. (2016) DNA Polymerase Conformational Dynamics and the Role of Fidelity-Confering Residues: Insights from Computational Simulations. *Front. Mol. Biosci.* 3, 20.

- (21) Moustafa, I. M., Shen, H., Morton, B., Colina, C. M., and Cameron, C. E. (2011) Molecular Dynamics Simulations of Viral RNA Polymerases Link Conserved and Correlated Motions of Functional Elements to Fidelity. *J. Mol. Biol.* 410, 159–181.

- (22) Euro, L., Haapanen, O., Róg, T., Vattulainen, I., Suomalainen, A., and Sharma, V. (2017) Atomistic Molecular Dynamics Simulations of Mitochondrial DNA Polymerase  $\gamma$ : Novel Mechanisms of Function and Pathogenesis. *Biochemistry* 56, 1227–1238.

- (23) Miller, B. R., Parish, C. A., and Wu, E. Y. (2014) Molecular Dynamics Study of the Opening Mechanism for DNA Polymerase I. *PLoS Comput. Biol.* 10, e1003961.

- (24) Kim, T., Freudenthal, B. D., Beard, W. A., Wilson, S. H., and Schlick, T. (2016) Insertion of oxidized nucleotide triggers rapid DNA polymerase opening. *Nucleic Acids Res.* 44, 4409–24.

- (25) Yang, L., Beard, W. A., Wilson, S. H., Broyde, S., and Schlick, T. (2002) Polymerase  $\beta$  simulations suggest that Arg258 rotation is a slow step rather than large subdomain motions per se. *J. Mol. Biol.* 317, 651–671.

- (26) Jia, L., Geacintov, N. E., and Broyde, S. (2008) The N-clasp of human DNA polymerase kappa promotes blockage or error-free bypass of adenine- or guanine-benzo[a]pyrenyl lesions. *Nucleic Acids Res.* 36, 6571–84.
- (27) Perera, L., Freudenthal, B. D., Beard, W. A., Pedersen, L. G., and Wilson, S. H. (2017) Revealing the role of the product metal in DNA polymerase  $\beta$  catalysis. *Nucleic Acids Res.*, gkw1363.
- (28) Shaik, M. M., Bhattacharjee, N., Feliks, M., Ng, K. K.-S., and Field, M. J. (2017) Norovirus RNA-dependent RNA polymerase: A computational study of metal-binding preferences. *Proteins: Struct., Funct., Genet.* 85, 1435.
- (29) Parks, J. M., Kondru, R. K., Hu, H., Beratan, D. N., and Yang, W. (2008) Hepatitis c virus ns5b polymerase: Qm/mm calculations show the important role of the internal energy in ligand binding. *J. Phys. Chem. B* 112, 3168–3176.
- (30) Carvalho, A. T. P., Fernandes, P. A., and Ramos, M. J. (2011) The Catalytic Mechanism of RNA Polymerase II. *J. Chem. Theory Comput.* 7, 1177–1188.
- (31) Warshel, A., and Levitt, M. (1976) Theoretical studies of enzymatic reactions: dielectric electrostatic and steric stabilization of the carbonium ion in the reaction of lysozyme. *J. Mol. Biol.* 103, 227–249.
- (32) Florián, J., Goodman, M. F., and Warshel, A. (2002) Theoretical Investigation of the Binding Free Energies and Key Substrate-Recognition Components of the Replication Fidelity of Human DNA Polymerase  $\beta$ . *J. Phys. Chem. B* 106, 5739–5753.
- (33) Florián, J., Warshel, A., and Goodman, M. F. (2002) Molecular Dynamics Free-Energy Simulations of the Binding Contribution to the Fidelity of T7 DNA Polymerase. *J. Phys. Chem. B* 106, 5754–5760.
- (34) Florián, J., Goodman, M. F., and Warshel, A. (2005) Computer simulations of protein functions: Searching for the molecular origin of the replication fidelity of DNA polymerases. *Proc. Natl. Acad. Sci. U. S. A.* 102, 6819–6824.
- (35) Radhakrishnan, R., and Schlick, T. (2006) Correct and incorrect nucleotide incorporation pathways in DNA polymerase  $\beta$ . *Biochem. Biophys. Res. Commun.* 350, 521–529.
- (36) Bojin, M. D., and Schlick, T. (2007) A quantum mechanical investigation of possible mechanisms for the nucleotidyl transfer reaction catalyzed by DNA polymerase  $\beta$ . *J. Phys. Chem. B* 111, 11244–11252.
- (37) Wang, L., Yu, X., Hu, P., Broyde, S., and Zhang, Y. (2007) A water-mediated and substrate-assisted catalytic mechanism for *Sulfolobus solfataricus* DNA polymerase IV. *J. Am. Chem. Soc.* 129, 4731–4737.
- (38) Schlick, T., Arora, K., Beard, W. A., and Wilson, S. H. (2012) Perspective: pre-chemistry conformational changes in DNA polymerase mechanisms. *Theor. Chem. Acc.* 131, 1287.
- (39) Kamerlin, S. C. L., Sharma, P. K., Prasad, R. B., and Warshel, A. (2013) Why nature really chose phosphate. *Q. Rev. Biophys.* 46, 1–132.
- (40) Rosta, E., Yang, W., and Hummer, G. (2014) Calcium Inhibition of Ribonuclease H1 Two-Metal Ion Catalysis. *J. Am. Chem. Soc.* 136, 3137–3144.
- (41) Perera, L., Freudenthal, B. D., Beard, W. A., Shock, D. D., Pedersen, L. G., and Wilson, S. H. (2015) Requirement for transient metal ions revealed through computational analysis for DNA polymerase going in reverse. *Proc. Natl. Acad. Sci. U. S. A.* 112, E5228–E5236.
- (42) Wang, Y., and Schlick, T. (2008) Quantum Mechanics/Molecular Mechanics Investigation of the Chemical Reaction in Dpo4 Reveals Water-Dependent Pathways and Requirements for Active Site Reorganization. *J. Am. Chem. Soc.* 130, 13240–13250.
- (43) Lior-Hoffmann, L., Wang, L., Wang, S., Geacintov, N. E., Broyde, S., and Zhang, Y. (2012) Preferred WMSA catalytic mechanism of the nucleotidyl transfer reaction in human DNA polymerase  $\kappa$  elucidates error-free bypass of a bulky DNA lesion. *Nucleic Acids Res.* 40, 9193–205.
- (44) Cisneros, G. A. (2012) Application of Gaussian Electrostatic Model (GEM) Distributed Multipoles in the Force Field. *J. Chem. Theory Comput.* 12, 5072–5080.
- (45) Starovoytov, O. N., Torabifard, H., and Cisneros, G. A. (2014) Development of AMOEBA Force Field for 1, 3-Dimethylimidazolium Based Ionic Liquids. *J. Phys. Chem. B* 118, 7156–7166.
- (46) Torabifard, H., Starovoytov, O. N., Ren, P., and Cisneros, G. A. (2015) Development of an AMOEBA water model using GEM distributed multipoles. *Theor. Chem. Acc.* 134, 1–10.
- (47) Karttunen, M., Rottler, J., Vattulainen, I., and Sagui, C. (2008) Computational Modeling of Membrane Bilayers. *Current Topics in Membranes*, Vol. 60, pp 49–89, Elsevier Inc.
- (48) Warshel, A., Kato, M., and Pliaskov, A. V. (2007) Polarizable Force Fields: History, Test Cases, and Prospects. *J. Chem. Theory Comput.* 3, 2034–2045.
- (49) Boulanger, E., and Thiel, W. (2012) Solvent Boundary Potentials for Hybrid QM/MM Computations Using Classical Drude Oscillators: A Fully Polarizable Model. *J. Chem. Theory Comput.* 8, 4527–4538.
- (50) Chaudret, R., Gresh, N., Narth, C., Lagardere, L., Darden, T. A., Cisneros, G. A., and Piquemal, J.-P. (2014) S/G-1: An ab Initio Force-Field Blending Frozen Hermite Gaussian Densities and Distributed Multipoles. Proof of Concept and First Applications to Metal Cations. *J. Phys. Chem. A* 118, 7598–7612.
- (51) Chaudret, R., Ulmer, S., van Severen, M.-C., Gresh, N., Parisel, O., Cisneros, G. A., Darden, T. A., Piquemal, J.-P., et al. (2008) Progress Towards Accurate Molecular Modeling of Metal Complexes Using Polarizable Force Fields. *AIP Conf. Proc.* 1102, 185–192.
- (52) Lamoureux, G., Harder, E., Vorobyov, I., Roux, B., and MacKerell, A. (2006) A polarizable model of water for molecular dynamics simulations of biomolecules. *Chem. Phys. Lett.* 418, 245–249.
- (53) Beese, L. S., and Steitz, T. A. (1991) Structural basis for the 3'-5' exonuclease activity of *Escherichia coli* DNA polymerase I: a two metal ion mechanism. *EMBO J.* 10, 25–33.
- (54) Fang, D., Chaudret, R., Piquemal, J.-P., and Cisneros, G. A. (2013) Toward a Deeper Understanding of Enzyme Reactions Using the Coupled ELF/NCI Analysis: Application to DNA Repair Enzymes. *J. Chem. Theory Comput.* 9, 2156–2160.
- (55) Lin, P., Pedersen, L. C., Batra, V. K., Beard, W. A., Wilson, S. H., and Pedersen, L. G. (2006) Energy analysis of chemistry for correct insertion by DNA polymerase  $\beta$ . *Proc. Natl. Acad. Sci. U. S. A.* 103, 13294–13299.
- (56) Cisneros, G. A., Perera, L., García-Díaz, M., Bebenek, K., Kunkel, T. A., and Pedersen, L. G. (2008) Catalytic mechanism of human DNA polymerase  $\lambda$  with  $Mg^{2+}$  and  $Mn^{2+}$  from *ab initio* quantum mechanical/molecular mechanical studies. *DNA Repair* 7, 1824–1834.
- (57) Sirover, M. A., and Loeb, L. A. (1976) Infidelity of DNA synthesis in vitro: Screening for potential metal mutagens or carcinogens. *Science* 194, 1434–1436.
- (58) Blanca, G., Shevelev, I., Ramadan, K., Villani, G., Spadari, S., Hübscher, U., and Maga, G. (2003) Human DNA polymerase  $\lambda$  diverged in evolution from DNA polymerase  $\beta$  toward specific  $Mn^{+2}$  dependence: a kinetic and thermodynamic study. *Biochemistry* 42, 7467–7476.
- (59) Fowler, J. D., Brown, J. A., Kvaratskhelia, M., and Suo, Z. (2009) Probing conformational changes of human DNA polymerase lambda using mass spectrometry-based protein footprinting. *J. Mol. Biol.* 390, 368–79.
- (60) Bebenek, K., Garcia-Diaz, M., Zhou, R.-Z., Povirk, L. F., and Kunkel, T. A. (2010) Loop 1 modulates the fidelity of DNA polymerase lambda. *Nucleic Acids Res.* 38, 5419–31.
- (61) Brenowitz, S., Kwack, S., Goodman, M. F., O'Donnell, M., and Echols, H. (1991) Specificity and enzymatic mechanism of the editing exonuclease of *Escherichia coli* DNA polymerase III. *J. Biol. Chem.* 266, 7888–7892.
- (62) McHenry, C. S. (1991) DNA polymerase III holoenzyme. *J. Biol. Chem.* 266, 19127–19130.
- (63) Cisneros, G. A., Perera, L., Schaaper, R. M., Pedersen, L. C., London, R. E., Pedersen, L. G., and Darden, T. A. (2009) Reaction mechanism of the  $\epsilon$  subunit of *E. coli* DNA polymerase III: insights



into active site metal coordination and catalytically significant residues. *J. Am. Chem. Soc.* 131, 1550–1556.

(64) Schaaper, R. M. (1993) Base selection, proofreading, and mismatch repair during DNA replication in *Escherichia coli*. *J. Biol. Chem.* 268, 23762–23765.

(65) Derbyshire, V., Pinsonneault, J. K., and Joyce, C. M. (1995) Structure-function analysis of 3'-5' exonuclease of DNA polymerases. *Methods Enzymol.* 262, 363–385.

(66) Hamdan, S., Bulloch, E. M., Thompson, P. R., Beck, J. L., Yang, J. Y., Crowther, J. A., Lilley, P. E., Carr, P. D., Ollis, D. L., Brown, S. E., and Dixon, N. E. (2002) Hydrolysis of the 5'-p-nitrophenyl ester of TMP by the proofreading exonuclease ( $\epsilon$ ) subunit of *Escherichia coli* DNA polymerase III. *Biochemistry* 41, 5266–5275.

(67) Cisneros, G. A., Perera, L., Schaaper, R. M., Pedersen, L. C., London, R. E., Pedersen, L. G., and Darden, T. A. (2009) Reaction Mechanism of the  $\epsilon$  Subunit of *E. coli* DNA Polymerase III: Insights into Active Site Metal Coordination and Catalytically Significant Residues. *J. Am. Chem. Soc.* 131, 1550–1556.

(68) Taft-Benz, S. A., and Schaaper, R. M. (2004) The  $\theta$  subunit of *Escherichia coli* DNA polymerase III: a role in stabilizing the  $\epsilon$  proofreading subunit. *J. Bacteriol.* 186, 2774–2780.

(69) Chikova, A. K., and Schaaper, R. M. (2005) The bacteriophage P1 *hot* gene product can substitute for the *Escherichia coli* DNA polymerase III  $\theta$  subunit. *J. Bacteriol.* 187, 5528–5536.

(70) Kirby, T. W., Harvey, S., DeRose, E. F., Chalov, S., Chikova, A. K., Perrino, F. W., Schaaper, R. M., London, R. E., and Pedersen, L. C. (2006) Structure of the *E. coli* DNA polymerase III  $\epsilon$ -HOT proofreading complex. *J. Biol. Chem.* 281, 38466–38471.

(71) Yang, W., Lee, J. Y., and Nowotny, M. (2006) Making and breaking nucleic acids: Two-Mg<sup>2+</sup>-Ion catalysis and substrate specificity. *Mol. Cell* 22, 5–13.

(72) Rosta, E., Nowotny, M., Yang, W., and Hummer, G. (2011) Catalytic Mechanism of RNA Backbone Cleavage by Ribonuclease H from Quantum Mechanics/Molecular Mechanics Simulations. *J. Am. Chem. Soc.* 133, 8934–8941.

(73) Gillet, N., Chaudret, R., Contreras-García, J., Yang, W., Silvi, B., and Piquemal, J.-P. (2012) Coupling Quantum Interpretative Techniques: Another Look at Chemical Mechanisms in Organic Reactions. *J. Chem. Theory Comput.* 8, 3993–3997.

(74) Nakamura, T., Zhao, Y., Yamagata, Y., Hua, Y.-J., and Yang, W. (2012) Watching {DNA} Polymerase  $\nu$  make a phosphodiester bond. *Nature* 487, 196–201.

(75) Freudenthal, B., Beard, W., Shock, D., and Wilson, S. (2013) Observing a {DNA} Polymerase Choose Right from Wrong. *Cell* 154, 157–168.

(76) Kratz, E. G., Walker, A. R., Lagardère, L., Lipparini, F., Piquemal, J.-P., and Andres Cisneros, G. (2016) LICHEM: A QM/MM program for simulations with multipolar and polarizable force fields. *J. Comput. Chem.* 37, 1019–1029.

(77) Genna, V., Vidossich, P., Ippoliti, E., Carloni, P., and De Vivo, M. (2016) A Self-Activated Mechanism for Nucleic Acid Polymerization Catalyzed by DNA/RNA Polymerases. *J. Am. Chem. Soc.* 138, 14592–14598.

(78) Hartwig, A. (1998) Carcinogenicity of metal compounds: possible role of DNA repair inhibition. *Toxicol. Lett.* 102–103, 235–239.

(79) Pelletier, H., Sawaya, M. R., Wolffe, W., Wilson, S. H., and Kraut, J. (1996) A structural basis for metal ion mutagenicity and nucleotide selectivity in human DNA polymerase  $\beta$ . *Biochemistry* 35, 12762–12777.

(80) Chaudret, R., Piquemal, J.-P., and Andres Cisneros, G. (2011) Correlation between electron localization and metal ion mutagenicity in DNA synthesis from QM/MM calculations. *Phys. Chem. Chem. Phys.* 13, 11239–11247.

(81) Joyce, C. M., and Grindley, N. D. (1984) Method for determining whether a gene of *Escherichia coli* is essential: application to the *polA* gene. *J. Bacteriol.* 158, 636–643.

(82) Bermek, O., Grindley, N. D. F., and Joyce, C. M. (2010) Distinct roles of the active site Mg<sup>2+</sup> ligands, D882 and L705 of DNA

polymerase I (Klenow Fragment) during the prechemistry conformational transitions. *J. Biol. Chem.* 286, 3755.

(83) Singh, K., and Modak, M. J. (2003) Presence of 18-Å long hydrogen bond track in the active site of *Escherichia coli* DNA polymerase I (Klenow Fragment): Its requirement in the stabilization of enzyme-template-primer complex. *J. Biol. Chem.* 278, 11289–11302.

(84) Kuchta, R. D., Benkovic, P., and Benkovic, S. J. (1988) Kinetic mechanism whereby DNA polymerase I (Klenow) replicates DNA with high fidelity. *Biochemistry* 27, 6716–6725.

(85) Beese, L. S., Friedman, J. M., and Steitz, T. A. (1993) Crystal structures of the Klenow fragment of DNA polymerase I complexed with deoxynucleoside triphosphate and pyrophosphate. *Biochemistry* 32, 14095–14101.

(86) Freemont, P. S., Friedman, J. M., Beese, L. S., Sanderson, M. R., and Steitz, T. A. (1988) Cocrystal structure of an editing complex of Klenow fragment with DNA. *Proc. Natl. Acad. Sci. U. S. A.* 85, 8924–8928.

(87) Singh, K., and Modak, M. J. (2005) Contribution of Polar Residues of the J-Helix in the 3'-5' exonuclease activity of *Escherichia coli* DNA polymerase I (Klenow fragment): Q677 regulates the removal of terminal mismatch. *Biochemistry* 44, 8101–8110.

(88) Thompson, E. H. Z., Bailey, M. F., van der Schans, E. J. C., Joyce, C. M., and Millar, D. P. (2002) Determinants of DNA Mismatch Recognition within the Polymerase Domain of the Klenow Fragment. *Biochemistry* 41, 713–722.

(89) Minnick, D. T., Bebenek, K., Osheroff, W. P., Turner, R. M., Astatke, M., Liu, L., Kunkel, T. A., and Joyce, C. M. (1999) Side Chains That Influence Fidelity at the Polymerase Active Site of *Escherichia coli* DNA Polymerase I (Klenow Fragment). *J. Biol. Chem.* 274, 3067–3075.

(90) Bebenek, K., Joyce, C. M., Fitzgerald, M., and Kunkel, T. A. (1990) The fidelity of DNA synthesis catalyzed by derivatives of *Escherichia coli* DNA polymerase I. *J. Biol. Chem.* 265, 13878–13887.

(91) Loh, E., and Loeb, L. E. (2005) Mutability of DNA polymerase I: Implications for the creation of mutant DNA polymerases. *DNA Repair* 4, 1390–1398.

(92) Christian, T., Romano, L., and Rueda, D. (2009) Single-molecule measurements of synthesis by DNA polymerase with base-pair resolution. *Proc. Natl. Acad. Sci. U. S. A.* 106, 21109–21114.

(93) Graham, S. E., Syeda, F., and Cisneros, G. A. (2012) Computational Prediction of Residues Involved in Fidelity Checking for DNA Synthesis in DNA Polymerase I. *Biochemistry* 51, 2569–2578.

(94) Elias, A. A., and Cisneros, G. A. (2014) Chapter Two-Computational Study of Putative Residues Involved in DNA Synthesis Fidelity Checking in *Thermus aquaticus* DNA Polymerase I. *Adv. Protein Chem. Struct. Biol.* 96, 39–75.

(95) Florián, J., Goodman, M. F., and Warshel, A. (2003) Computer simulation of the chemical catalysis of DNA polymerases: Discriminating between alternative nucleotide insertion mechanisms for T7 DNA polymerase. *J. Am. Chem. Soc.* 125, 8163–8177.

(96) Florián, J., Goodman, M. F., and Warshel, A. (2005) Computer simulations of protein functions: Searching for the molecular origin of the replication fidelity of DNA polymerases. *Proc. Natl. Acad. Sci. U. S. A.* 102, 6819–6824.

(97) Johnson, E. R., Keinan, S., Mori-Sanchez, P., Contreras-Garcia, J., Cohen, A. J., and Yang, W. (2010) Revealing Noncovalent Interactions. *J. Am. Chem. Soc.* 132, 6498–6506.

(98) Contreras-García, J., Johnson, E. R., Keinan, S., Chaudret, R., Piquemal, J.-P., Beratan, D. N., and Yang, W. (2011) NCIPLOT: A Program for Plotting Noncovalent Interaction Regions. *J. Chem. Theory Comput.* 7, 625.

(99) Gelboin, H. V. (1980) Benzo[ $\alpha$ ]pyrene metabolism, activation and carcinogenesis: role and regulation of mixed-function oxidases and related enzymes. *Physiol. Rev.* 60, 1107–66.

(100) Ling, H., Sayer, J. M., Plosky, B. S., Yagi, H., Boudsocq, F., Woodgate, R., Jerina, D. M., and Yang, W. (2004) Crystal structure of a benzo[ $a$ ]pyrene diol epoxide adduct in a ternary complex with a DNA polymerase. *Proc. Natl. Acad. Sci. U. S. A.* 101, 2265–2269.

(101) Liyanage, P. S., Walker, A. R., Brenlla, A., Cisneros, G. A., Romano, L. J., and Rueda, D. (2017) Bulky Lesion Bypass Requires Dpo4 Binding in Distinct Conformations (in preparation).

(102) Makridakis, N. M., and Reichardt, J. K. V. (2012) Translesion DNA polymerases and cancer. *Front. Genet.* 3, 174.

(103) Glick, E., White, L. M., Elliott, N. A., Berg, D., Kiviat, N. B., and Loeb, L. A. (2006) Mutations in DNA polymerase  $\eta$  are not detected in squamous cell carcinoma of the skin. *Int. J. Cancer* 119, 2225–2227.

(104) Swett, R. J., Elias, A., Miller, J. A., Dyson, G. E., and Andres Cisneros, G. (2013) Hypothesis driven single nucleotide polymorphism search (HyDn-SNP-S). *DNA Repair* 12, 733–740.

(105) Bebenek, K., Garcia-Diaz, M., Zhou, R.-Z., Povirk, L. F., and Kunkel, T. A. (2010) Loop 1 modulates the fidelity of DNA polymerase  $\lambda$ . *Nucleic Acids Res.* 38, 5419–5431.

(106) Terrados, G., Capp, J.-P., Canitrot, Y., García-Díaz, M., Bebenek, K., Kirchhoff, T., Villanueva, A., Boudsocq, F., Bergoglio, V., Cazaux, C., Kunkel, T. A., Hoffmann, J.-S., and Blanco, L. (2009) Characterization of a natural mutator variant of human DNA polymerase  $\lambda$  which promotes chromosomal instability by compromising NHEJ. *PLoS One* 4, e7290.

(107) Nemecek, A. A., Bush, K. B., Towle-Weicksel, J. B., Taylor, B. F., Schulz, V., Weidhaas, J. B., Tuck, D. P., and Sweasy, J. B. (2016) Estrogen Drives Cellular Transformation and Mutagenesis in Cells Expressing the Breast Cancer-Associated R438W DNA Polymerase Lambda Protein. *Mol. Cancer Res.* 14, 1068–1077.